The influence of geogenic and anthropogenic factors on indoor radon exposure in the Ervedosa ore district (Vinhais - Northeastern Portugal)

Maria E. P. Gomes[1,3], Lisa M. O. Martins[2,4] & Alcides, J. S. C. Pereira[5]

[1] University of Trás-os-Montes e Alto Douro, Department of Geology, Quinta de Prados, P-5000 801 Vila Real, Portugal. E-mail: mgomes@utad.pt

[2] University of Coimbra, Faculty of Sciences and Technology, Department of Earth Sciences, Polo II, Rua Sílvio Lima, P-3000 272 Coimbra, Portugal

[3] University of Coimbra, Geosciences Center, P-3000 272 Coimbra, Portugal

[4] Centre for the Research and Technology of Agro-Environment and Biological Science, Vila Real, Portugal. E-mail: lisa_martins@hotmail.com

[5] University of Coimbra, Centre for Earth and Space Research of the University of Coimbra, Faculty of Sciences and Technology, Department of Earth Sciences, Polo II, Rua Sílvio Lima, P-3000 272 Coimbra, Coimbra, Portugal. E-mail:apereira@dct.uc.pt

Abstract: The Ervedosa ore district lies in the Galiza and Trás-os-Montes Zone. The schist S1 is dominated by low-grade metamorphism, and schist S2 occurs along or close to the uranium mineralized area with secondary minerals along the schistosity plane. These metamorphic rocks are intruded by a syn-tectonic Variscan granite pluton with an elongated form, constrained by the NW-SE Rebordelo (RE) ductile shear zone. Geochemical and radiological data obtained in the three localities of the Ervedosa village suggest that the radon concentrations in dwellings are mainly related to the uranium content of rocks and their mobilization through weathering processes, but human habits also have a role on it. The Ervedosa Mine (EM) granite, presents the highest average of uranium concentration (14 ppm). The results of the gamma dose rate are related to the uranium contents of the rocks and weathering processes. Thus, radon risk exposure is moderate to high in dwellings located in EM granite and schist S2, and low for RE granite and schist S1. Overall, radon concentrations determined in 46 dwellings during winter conditions shown a geometric mean of 257.1 $Bq \cdot m^{-3}$. Therefore 32% of

Abrantes, I., Callapez, P. M., Correia, G. P., Gomes, E., Lopes, B., Lopes, F. C., Pires, E., & Rola, A. (Eds.), *Uma visão holística da Terra e do Espaço nas suas vertentes naturais e humanas. Homenagem à Professora Celeste Romualdo Gomes*. Coimbra: CITEUC.
 DOI: http://doi.org/10.5281/zenodo.4409304

measurements exceeded the 300 Bq.m^{-3} reference limit, by the DL n.º108/2018. The present study alert for human health risks from indoor radon exposure and also recommend preventive and corrective measures in this region. Awareness campaigns for public should also be improved to ensure natural ventilation in dwellings during the winter period and reduce the indoor radon exposure.

Keywords: Granites, Human habits, Indoor radon, Schists, Structural control, Weathering processes.

Resumo: *O distrito mineiro da Ervedosa situa-se na Zona da Galiza e Trás-os-Montes. O xisto S1 é dominado por metamorfismo de baixo grau, e o xisto S2 ocorre próximo da área mineralizada de urânio com minerais secundários ao longo do plano de xistosidade. Nestas rochas metamórficas ocorre a intrusão de um plutão granítico varisco e sintectónico de forma alongada, controlado pela zona de cisalhamento dúctil NW-SE Rebordelo (RE). Dados geoquímicos e radiológicos obtidos nas três localidades de Ervedosa sugerem que as concentrações de radão nas habitações se encontram relacionadas com o teor de uranio das rochas e sua mobilização através de processos de alteração, assim como também pelos hábitos humanos. O granito da mina de Ervedosa (EM) apresenta a maior concentração média de uranio (14 ppm). Os resultados da taxa de dose de radiação gama também se encontram relacionados com o conteúdo de urânio das rochas e com os processos de intemperismo. Assim, a exposição ao risco de radão é moderada a alta em habitações localizadas no granito EM e xisto S2, e baixa no granito RE e xisto S1. Em geral, as concentrações de radão determinadas para 46 residências durante o período de inverno mostraram uma média geométrica de 257.1 Bq·m-3. Desta forma, 32% das medições excederam o limite de referência de 300 Bq·m-3, pelo DL nº 108/2018. O presente estudo alerta para os riscos na saúde humana decorrentes da exposição ao radão em espaços confinados e também recomenda medidas preventivas e corretivas nesta região. Campanhas de sensibilização para os cidadãos devem ser asseguradas para garantir a ventilação natural nas residências durante o período de inverno e reduzir a exposição ao radão.*

Palavras-chave: *Granitos, Hábitos humanos, Radão interior, Xistos, Controle estrutural, Processos de alteração.*

Introduction

Radon is a colourless, odourless and tasteless inert gas with a half-life of 3.8 days, naturally formed from the radioactive decay of elements of the uranium series, which is found in small quantities in rocks and soils, as well as in building construction materials (Darby et al., 2005). Radon and some of its progeny decay with the emission of an alpha particle, and if in high concentrations and inhaled for a long time may induce lung cancer. It is the second most important risk factor for lung cancer after smoking (EPA 2003; Darby et al., 2005; WHO, 2010). Recent epidemiological studies on indoor radon and lung cancer in Europe, North America and Asia, provide strong evidence that radon causes a substantial number of lung cancers in the general population, The risk rises 16 % for every 100 Bq/m^3 increase in residential concentrations (Darby et al., 2005).

The primary source of indoor radon is the underlying soil, but the building materials can also contribute to radon exposure. The indoor radon level is influenced by the radium content in the soils

but also by permeability and building ventilation systems (natural *versus* mechanical air exchange) (BEIR VI, 1999; WHO, 2010). Therefore, indoor radon accumulation could be controlled by a large number of geogenic and anthropogenic features (Cosma et al., 2013; 2015), such as geology, soil properties, climate, the building materials, the architecture of the buildings, ventilation systems and the lifestyle habits of the inhabitants (Talavera et al., 2013).

Concerning the geological factors, it is currently accepted that in the granitic rocks are the lithology that has the highest geogenic radon potential. Nevertheless, this potential can vary a lot between the different types of granites (Pereira et al., 2017). The geochemical composition, the petrography, namely the location of the parent uranium in the minerals, as well as secondary features related to post-crystallization processes, inducing the leaching of uranium from its bearing minerals and redeposition in the alteration zones or other surrounding lithologies, usually linked to metamorphic aureole or faults, are factors that often have been pointed out to explain the variability of the radon potential in plutonic or metamorphic rocks. Still, the mechanisms involved are not yet fully understood.

The weathering indices have been widely used in several studies and applied in heterogeneous plutonic and metamorphic rocks to understand the weathering impact on physical properties of rocks, climate changes on bedrock alteration and mobility of critical elements during the rock-soil interface, among others (Nesbitt & Young, 1984; Sharma & Rajamani, 2000; Dupré et al., 2003; Price & Velbel, 2003; Beaulieu et al., 2012; Domingos & Pereira, 2018). This study was carried out in Northern Portugal, to help and improve the knowledge about the correlation between indoor radon and the geogenic and anthropogenic variables, in and around the ore district of Ervedosa. It is therefore essential to understand the impact of all these factors on exposure to indoor radon and human health.

Geological setting

The Ervedosa area, Northern Portugal is situated in the Galiza -Trás-os-Montes Zone within the imbricated margins of the Iberian Terrane (Ribeiro, 1990). It belongs to the lower of the parautochthonous domain that consists mainly of mica schists and quartzites, deformed by three tectonic deformation phases D1, D2 and D3. These terrains have a low grade of regional metamorphism with a maximum temperature of 450 °C and pressure 6-7 kb (Lécolle et al., 1981).

At south Ervedosa village, a syn-tectonic Variscan biotite granite pluton outcrops, with an elongated form constrained by the NW-SE Rebordelo ductile shear zone. This granite has a medium- to coarse-grained porphyritic biotite-muscovite granite (Rebordelo (RE) granite, with 347 ± 9 Ma, showing sharp contacts with metasediments (Gomes & Neiva, 2005). Three Hercynian highly peraluminous granites define a sequence ranging from muscovite-biotite granite to muscovite granite (Gomes & Neiva, 2002). Tin-bearing quartz veins are genetically related to this sequence and were exploited in the Ervedosa-Tuela mine. The fine- to medium-grained muscovite tin-bearing granite (Ervedosa Mine (EM) granite,) is intruded in the Upper Silurian to Lower Devonian metasedimentary

sequence of the country rocks (schist S1), which includes carbon-rich metasediments, in the core of a Hercynian antiform (Fig. 1a,b).

Ervedosa urban area is situated in the northeastern, near the contact of RE and schists S1. In the southeastern area, schist S2 have uranium-bearing minerals along the main foliation and a small mineral occurrence of uranium (Ervedosa 1453U) with U_3O_8 of 0,09 % (SIORMINP, in Portuguese). Schist S2 is classified as uraniferous schist because it contains more than 0.005 % of U_3O_8 (Young, 1984). Secondary uranium minerals occur in this uraniferous schist, such as torbernite, autunite and saleite disseminated close the granitoids contact within Argana fault zone. Soutilha locality is situated in EM granite, near the N-S fault zone, and Falgueiras is located in the parautochtonous metasedimentary rocks S1 (Fig. 1b).

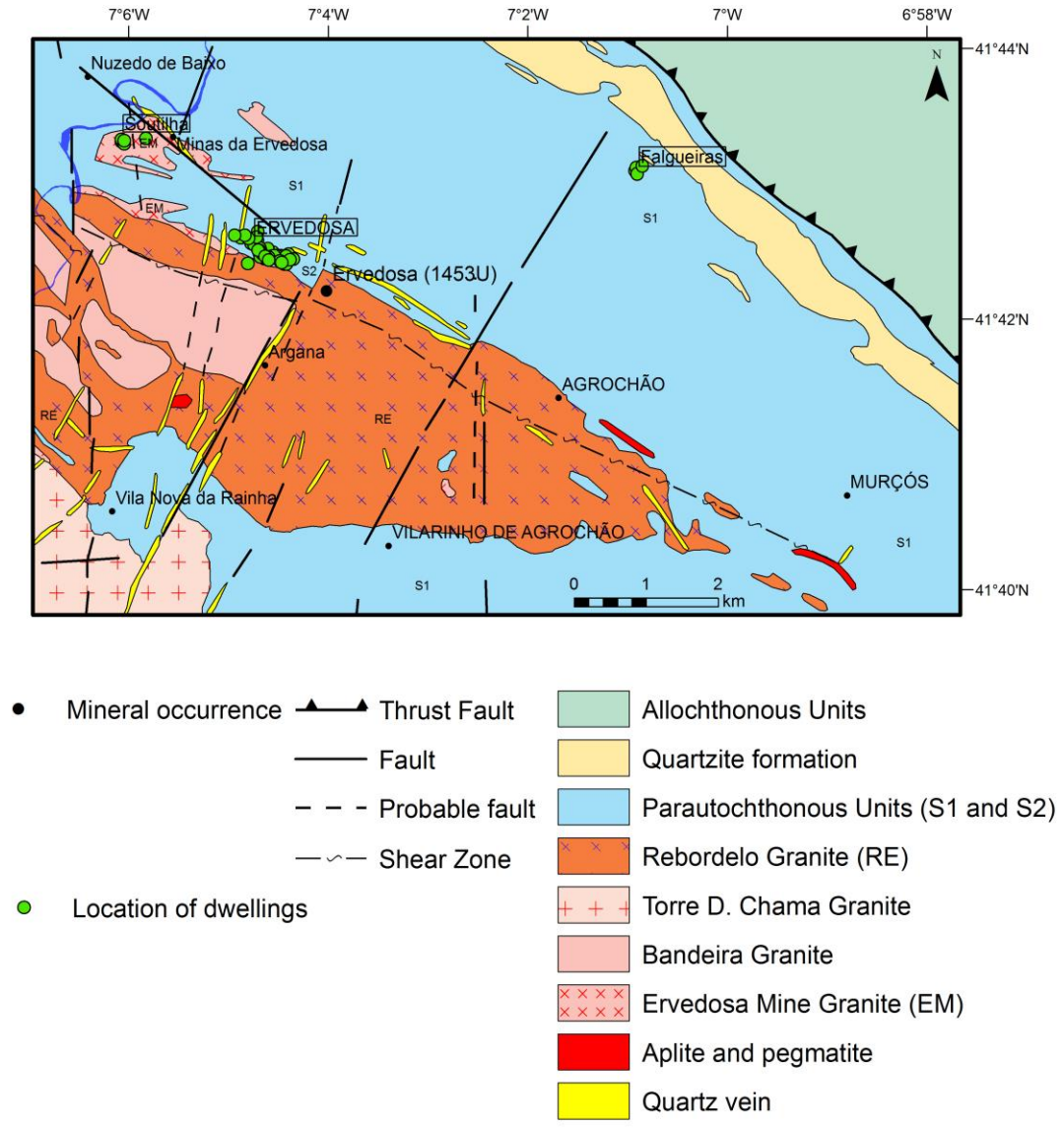

Figure 1 - Geological simplified map of Ervedosa ore area and the localities of Ervedosa, Soutilha and Falgueiras.

Materials and methods

The petrographic studies of thin polished sections of non-altered granites and schists were carried out at the Department of Geology of University of Trás-os-Montes and Alto Douro, whereas the BSE imaging in granites was performed at Electronic Microscope Laboratory, University of Minho.

The major and trace elements of granites were determined by X-ray fluorescence (XRF) at Manchester University, using the method of Brown et al. (1973), with precisions better than ±1%. Uranium and thorium were determined by neutron activation at the Imperial College Reactor Center, Ascot, U.K., with an accuracy of about ±5 %.

As rocks present a variable grade of weathering, due to their dependence of bedrock source and alteration processes, several chemical ratios of weathering were computed using the geochemical data (i.e., PIA, CIW, CIA and WIP from Parker, 1970; Nesbitt & Young, 1982; Harnois, 1988; Fedo et al., 1995), respectively; Tab. I). CIA, CIW and PIA indices should increase as weathering processes occur, while WIP should decrease with enhanced weathering (Tab. I).

The evaluation of weathering progress was attempted through chemical indices, using geochemical data (Tab. I). The relationship between chemical proxies and radiological properties was performed using nonparametric statistical methods. As the weathering proxies could produce distinct indices for weathered and un-weathered rocks (Price & Velbel, 2003; Domingos & Pereira, 2018), it was intended to compare the different types of granites with the Mann-Whitney U test and total lithologies using Kruskal-Wallis test. The statistical analysis was performed with XLSTAT software (Version 2016.02.28451; Adinsoft, 2010). The statistical significance level was established for 0.05.

Table I - Chemical indices and ratios for weathering in rocks.

Weathering indices	Source	Formula
Weathering index (WIP)	Parker (1970)	$\frac{Al_2O_3}{Al_2O_3+CaO+Na_2O} \times 100$
Chemical index of Alteration (CIA)	Nesbit & Young (1982)	$\frac{Al_2O_3-K_2O}{Al_2O_3+CaO+Na_2O-K_2O} \times 100$
Chemical index of weathering (CIW)	Harnois (1988)	$\frac{2Na_2O}{0.35}+\frac{MgO}{0.9}+\frac{2K_2O}{0.25}+\frac{CaO}{0.7} \times 100$
Plagioclase index of Alteration (PIA)	Fedo et al. (1995)	$\frac{Al_2O_3}{Al_2O_3+CaO+Na_2O+K_2O} \times 100$

A portable GF Instruments γ-ray spectrometer, model Gamma Surveyor compact 2, equipped with a NaI detector was employed in the field radiometric survey, covering the two different granites and the contact metamorphosed rocks, with a total of 30 field measurements. The spectrometer was set close to the surface of rock or soil, and then three measurements were done for three minutes each. The final value resulted from the average of those three measurements.

Suitable fracture networks promote the transport of radon from the rocks to the surface. The rock matrix may incorporate uranium accessory minerals that under weathering conditions, may trigger the leaching and precipitation of uranium mineralizations. For an evaluation of the fracturing network, a

two-step procedure of ESRI ArcMap (ESRI, 2010) was used to determine the distance from each indoor radon measurements to the nearest geological fault. In the first step, a shapefile of lines containing all regional faults was used as an input to the "Near" tool (second step). This previous tool is used to calculate the distance from each dwelling to the nearest fracture, producing in the attribute table of the sampling points (dwellings), the shortest distance to the adjacent geological fault.

Indoor radon concentrations were determined using CR-39 passive detectors in 46 dwellings built on different lithologies, during the winter. These passive radon detectors were placed on the ground floors and first floors of dwellings, and the period of exposure was about three months, between january and april of 2018. During this winter period, dwellings are less ventilated, and consequently, radon accumulates more easily than in the summer period. After the indoor exposure time, the CR-39 passive detectors were chemically etched with a NaOH solution, at a temperature of 90 ºC, and the track density was measured by image analysis system (Radosys) in the Laboratory of Natural Radioactivity of the University of Coimbra. The average analytical error is less than 15%.

.

Results and discussion

Geogenic control

Schist S1 contains quartz, K-feldspar, andaluzite, cordierite, muscovite, biotite, tourmaline, chlorite, monazite, apatite, zircon, ilmenite, rutile and rare variscite and uraninite. The RE granite contains quartz, microperthitic K-feldspar, plagioclase, biotite, titanite, apatite, ilmenite, zircon, monazite and rutile. Epidote and chlorite (after biotite) are rare. The EM granite contains quartz, K-feldspar, plagioclase, muscovite, and rare biotite, chlorite, monazite, apatite, zircon, ilmenite, rutile, columbite-tantalite and uraninite. Muscovite is subhedral and contains inclusions of quartz, sillimanite, zircon, apatite, ilmenite, monazite and rutile. In some localities of the studied area, the weathering of uranium-bearing granites may produce secondary uranium minerals on the border of the minerals, in microfractures and adjacent to major fracture systems within the parent pluton. Regional fractures and shear intersections could be considered favourable sites for transport and deposition of secondary uranium minerals. Thus, associated minerals may include uranium and thorium accessory minerals, especially monazite, apatite, titanite and zircon included in apatite in RE granite (Fig. 2a,d) and apatite, monazite, zircon, ilmenite, and uraninite in the EM granite (Fig. 2b,c). Rare and small uraninite was found in both RE and EM granites (Fig. 2b,e). In RE granite the monazite reaches up 9 % of ThO_2 and 1 % of UO_2 in its composition. Uraninite presents up 3 % of PbO and 4 % of ThO_2 in both granites RE and EM. Uranium can also be released by weathering processes in granites and migrate to low to medium grade metamorphic rocks around shallow-set plutons. This uranium mineralization and its mobility are similar to other uraniferous regions of the western Iberia: Nisa (Portugal), Vilariça (Moncorvo) and Ciudad Rodrigo (Spain) metallogenic provinces (Limpo de Faria, 1966; Pereira et al., 2015; Costa et al., 2017; Prazeres et al., 2018).

The whole-rock geochemical data and chemical compositions of minerals from this metallogenic area were used to understand the early granitoids petrogenesis, magmatic process, and specific involved AFC processes (Assimilation-fractional crystallization; Gomes & Neiva, 2002, 2005).

The weathering processes have substantial impacts on the chemical and physical properties of rocks. This processes can affect the content and distribution of uranium in the rocks, as well as increase their permeability. Uranium is very susceptible to transportation/leaching processes under post-magmatic/late hydrothermal and weathering conditions (Tartèse et al., 2013). Therefore, it is essential to evaluate the amount of remobilized uranium within the plutons and surrounding metamorphic rocks.

The chemical and radiological properties of metasediments and granites collected in the studied area are presented in table II. Despite the variable degree of weathering, the chemical composition of Fe_2O_3t, MnO, K_2O and P_2O_5 are similar for both granite types and metasediments. Hence, the compositional differences between granites and metasediments concerning MgO, CaO and Na_2O are mainly due to the geochemical nature of each bedrock source.

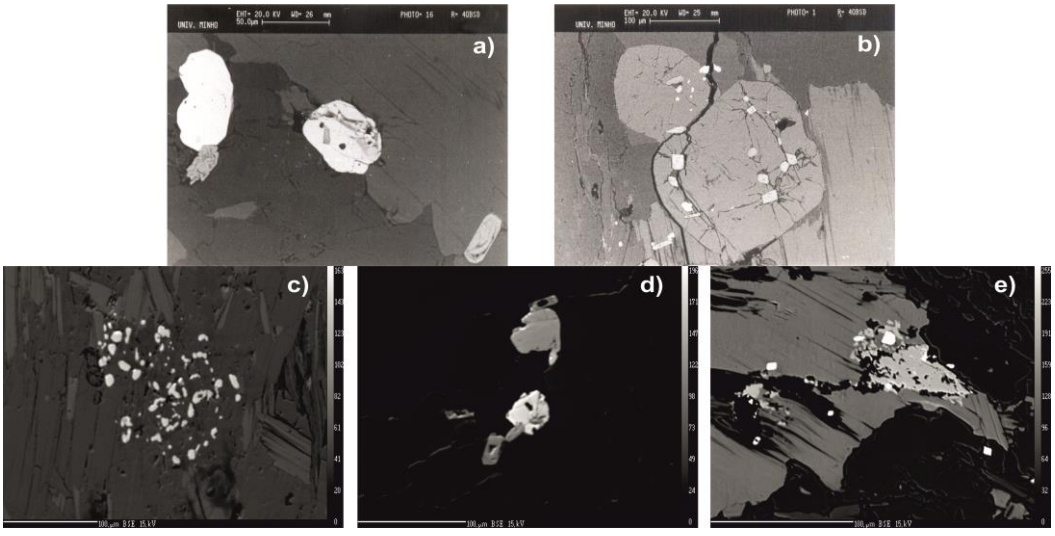

Figure 2 - Backscattered electron images of accessory minerals. a. Monazite and zircon included in apatite in RE granite. b. two apatite crystals with monazite, zircon, ilmenite and uraninite in the EM granite. c. apatite with inclusions of monazite and zircon in EM granite. d. apatite, zircon and monazite crystals in RE granite. e. muscovite with monazite, zircon, ilmenite and uraninite in the EM granite.

The CIA, CIW, and PIA indices increase, on average, from metasedimentary rocks, to the granites of the present study, whereas WIP decreases. According to the Mann-Whitney and Kruskal Wallis tests, the chemical indices WIP, CIA, and CIW are similar for both groups. Moreover, the opposite is true for PIA (Tab. I). Uranium content is similar between granites types whereas thorium and Th/U ratios are comparably lower in EM granite, though not statistically different for U and U-(Th/3.5)

Table II - Chemical composition, weathering proxies and radiological properties of studied lithologies.

Major elements	Sch S1 (n=3)				ME (n=6)				RE (n=6)				Mann-Whitney test (EM-RE)	Kruskal-Wallis test (Sch-EM-RE)
	Min.	Max.	AM	SD	Min.	Max.	AM	SD	Min.	Max.	AM	SD		
SiO_2	56.11	74.28	65.34	7.42	73.61	74.72	74.13	0.39	67.35	69.80	68.48	0.85	**0.002**	**0.019**
TiO_2	0.63	1.26	0.93	0.26	0.01	0.12	0.07	0.04	0.51	0.61	0.56	0.03	**0.005**	**0.015**
Al_2O_3	12.77	23.05	17.65	4.21	14.45	14.77	14.64	0.11	15.03	16.50	15.68	0.49	**0.005**	**0.015**
Fe_2O_3t	1.35	1.93	1.69	0.25	0.20	0.46	0.34	0.10	0.14	0.73	0.39	0.21	0.748	0.138
MnO	0.16	0.21	0.19	0.02	0.09	0.12	0.10	0.01	0.10	0.11	0.11	0.01	0.865	0.121
MgO	1.41	2.57	2.00	0.47	0.02	0.28	0.13	0.09	0.98	1.27	1.13	0.09	**0.002**	**0.016**
CaO	0.00	0.07	0.05	0.03	0.24	0.50	0.40	0.10	1.21	2.29	1.80	0.32	**0.005**	**0.015**
Na_2O	0.01	1.12	0.49	0.47	3.60	4.73	4.04	0.36	3.12	3.89	3.42	0.29	**0.030**	**0.038**
K_2O	3.46	5.88	4.59	0.99	2.93	4.57	4.06	0.58	3.13	5.74	4.67	0.81	0.128	0.232
P_2O_5	0.07	0.13	0.10	0.02	0.26	0.62	0.39	0.13	0.22	0.35	0.29	0.04	0.261	0.099
H_2O+	1.87	3.64	2.49	0.81	0.99	1.24	1.13	0.08	0.55	1.13	0.81	0.24	**0.030**	**0.038**
Total	99.50	100.34	100.03	0.37	99.86	100.23	100.05	0.11	99.26	100.58	99.98	0.39	0.575	0.271
A/CNK	2.24	3.58	3.03	0.57	1.21	1.29	1.25	0.03	1.11	1.15	1.13	0.02	**0.005**	**0.015**
Trace elements														
U	6.00	9.00	7.33	1.25	16.00	19.00	17.50	0.96	6.00	26.00	13.17	9.10	0.375	0.334
Th	10.00	17.00	14.33	3.09	5.00	9.00	6.17	1.46	14.00	29.00	20.50	5.80	**0.005**	**0.025**
Th/U	1.43	2.67	1.99	0.51	0.26	0.50	0.35	0.08	0.58	3.83	2.23	1.13	**0.002**	**0.032**
U-(Th/3.5)	1.43	4.14	3.24	1.28	14.57	17.57	15.74	0.92	-0.57	21.71	7.31	8.90	0.378	0.439
Chemical weathering proxies														
WIP	43.26	60.24	49.09	7.89	69.80	75.62	73.05	2.06	68.70	85.46	78.89	5.66	0.173	0.130
CIA	69.08	78.07	74.59	3.94	54.74	56.28	55.46	0.58	50.60	55.83	52.98	1.53	0.066	0.055
CIW	86.64	99.90	94.57	5.72	62.72	68.90	66.57	1.87	62.35	64.32	63.83	0.69	0.066	0.055
PIA	82.08	99.87	92.70	7.66	56.84	59.57	58.21	0.98	51.03	57.77	54.37	1.96	**0.031**	**0.039**

n – number of samples; Min – minimum; Max – maximum; AM – arithmetic mean; SD – standard deviation

between the two groups of granites and the three groups of studied rocks (Tab. II). As there was no increase of Th/U ratio above 4 (Fig. 3c), it is suggested according to Domingos & Pereira (2018) and McLennan et al. (1993) that there was no specific weathering event responsible for uranium removal, approaching the Th/U ratio close to the average Upper Continental Crust (UCC).

The thorium content and Th/U ratio stand out on RE granite and Schist S1, partly due to its geochemical signature ally to strong mobilization towards faults and shear zones. Furthermore, when Th/U ratio is disturbed, it may indicate a depletion or enrichment of uranium (Fawzy, 2017). In this study area, it is evident for EM and some samples of RE granite a decreasing of Th/U ratios accompanied by enrichment of uranium (Fig. 3b). The opposite is also true for some samples of RE granite, where thorium increases as the Th/U ratio decreases (Fig. 3c). However, the thorium content also increased in four samples of RE granite and Sch S1 with an increase in Th/U ratio and a decrease in uranium, which demonstrates a depletion of uranium that by secondary and dissemination processes may lead to the enrichment of uranium in Sch S2 (Figs. 3a,c e 4b).

It should also be noted that one sample of the RE granite reaches a negative value of uranium mobilization equation (U-(Th/3.5)=-0.6), which means once again the existence of some uranium leaching out (Fig. 3d e Tab. II). As Fawzy (2017) suggests, the uranium enrichment in EM and two samples of RE granites is proven through the increasing trend of U-(Th/3.5) (Fig. 3d). All these relationships found in U-Th, U-Th/U, Th-Th/U and U-(Th/3.5) diagrams present several crucial trends to prove the eventual mobilization and processes of redistribution of U from the granite RE to Sch S2 (Fig. 4b). The poor correlation between U and SiO_2 (Fig. 3e) may indicate a secondary source of uranium (Fawzy, 2017). The diagram U-Th/3.5 ratio versus SiO_2 also checks the leaching of uranium in four samples of RE granite and subsequent redistribution of uranium by the post magmatic processes (Fig. 3f). Thus, the uranium enrichment in two samples of RE granite may not only related to magmatic processes but also due to secondary dissemination processes. It is also important to mention that these samples were collected under the ductile shear zone.

According to Neiva & Matos Dias (2010) the uranium mineralizations within the Portuguese terrains of CIZ occur through the same behaviour and geological context of Alto Alentejo Uranium Province. Thus, these uranium deposits are usually hosted by granites creating disseminated uranium from contact with metamorphic aureoles, as occurs in this study area and other deposits of NE of Portugal (e.g., Horta da Vilariça). In addition, in this study area as well as in Alto Alentejo uranium province, uranium mineralizations may be present in faults and fractures in association with quartz filling (Ervedosa-1453U; Fig. 1). Prazeres et al. (2018) suggests that these weathered veins of deformed quartz with crystalline structure damage due to radiation released by uranium may become kinematically active within the granite, sometimes exhibiting alteration from previous hydrothermal events and even more recent weathering. As it occurs in the Nisa deposit, these faults tend to anastomose and penetrate the schist and spread uranium-bearing fluids over schistosity planes and wide related fractures.

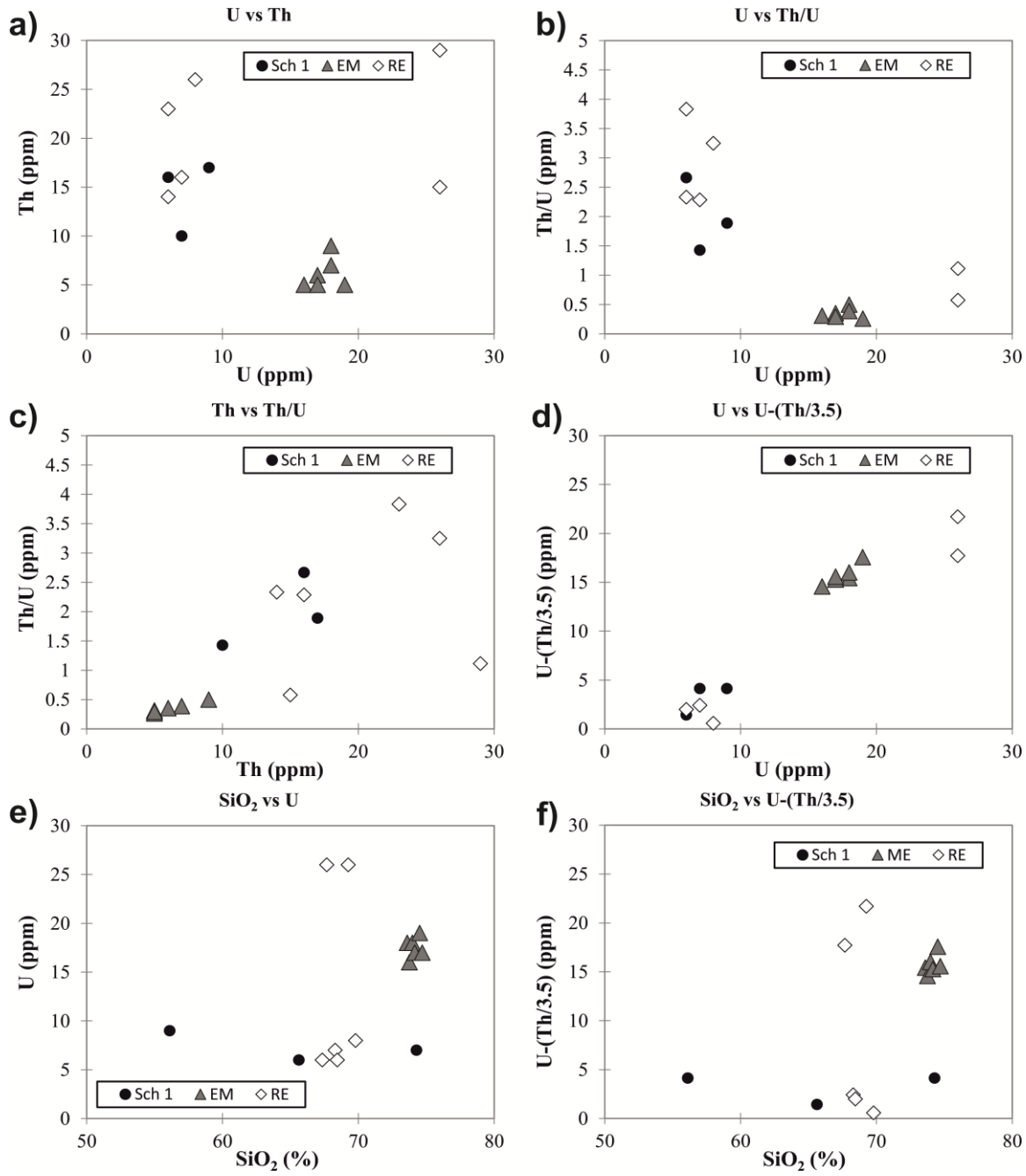

Figure 3 - Variation diagrams of S1 schist, RE and EM granites. a. the U versus Th. b. the U versus Th/U ratio. c. the Th versus Th/U ratio. d. U content versus uranium mobilization equation U-(Th/3.5). e. U versus SiO_2. f. uranium mobilization equation U-(Th/3.5) versus SiO_2.

The potassium, uranium and thorium contents measured in studied lithologies from Ervedosa ore province are higher than the crustal average (K- 2.1 %, U- 2.7 ppm and Th- 9.6 ppm; Fig. 4a-d). Uraniferous granites constitute a specific classification from Darnely (1982), and the best examples of uranium-rich granites are some Hercynian massifs of Portugal. The results obtained for these two

groups of muscovite-biotite granites suggest that specific gross compositional and weathering processes are indicative of genetically associated uranium mineralization (e.g. a high U/Th ratio combined with uranium levels above the crustal background, and the presence of uranium and thorium-bearing accessory minerals). The EM granite is a uraniferous granite, with several of these criteria, since their average uranium content is above 16 ppm (Darnley, 1982; Cambon, 1994). It is also a tin-bearing granite with magmatic fractionation responsible for the increase of Sn contents and their micas. The Ervedosa's tin quartz veins are genetically related to EM granite, where metals such as Sn and As were explored between 1939 and 1965 (Gomes & Neiva, 2002).

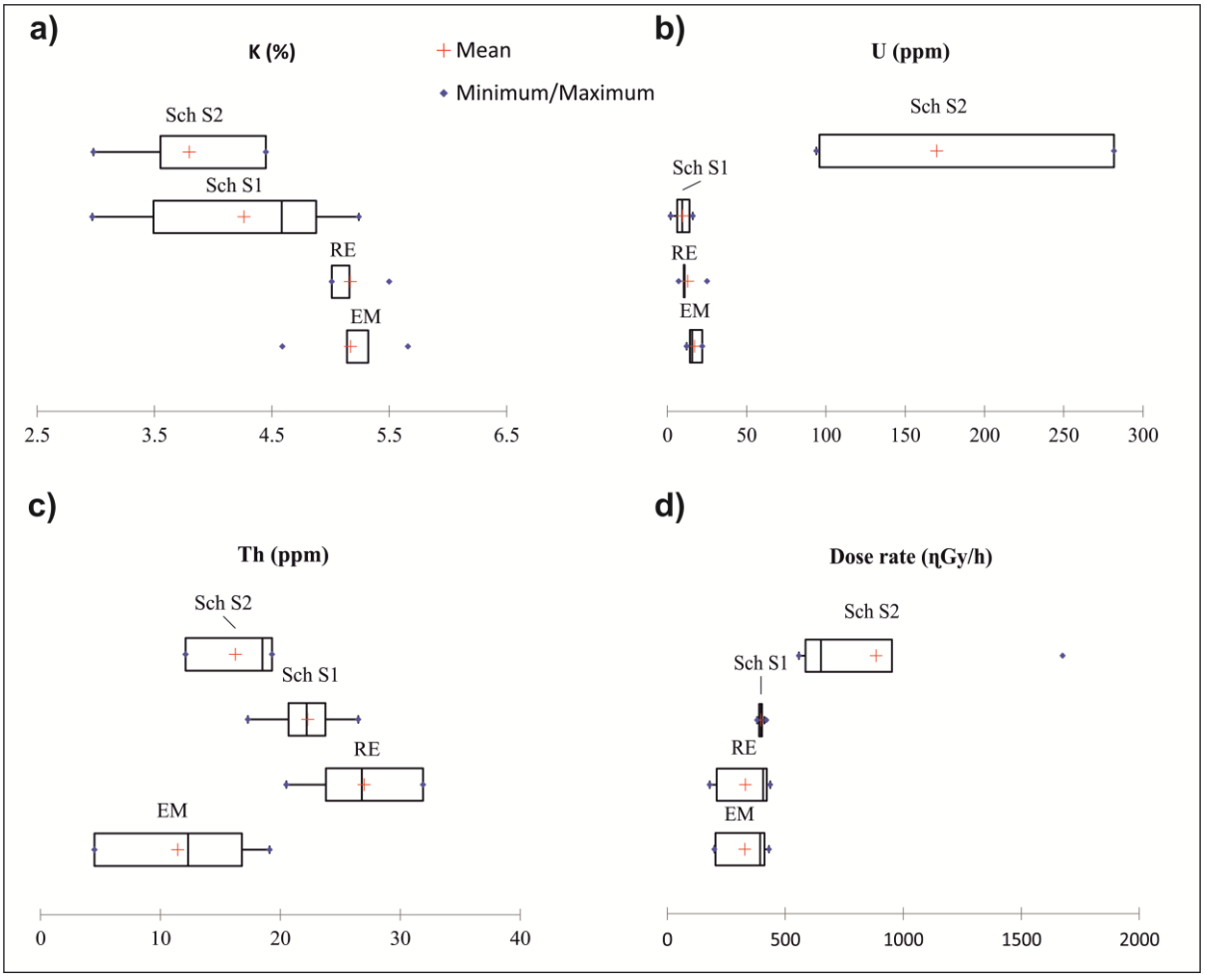

Figure 4 - Radiometric background for the Ervedosa ore district. a. K(%). b. U (ppm). c. Th (ppm). Dose rate (ηGy·h^{-1}).

The structural control for radon conduction in dwellings

In this region, the distances of uranium transport until reach the host rock are essentially governed by the permeability from bedrock (regional faults and microfractures) and effective porosity from

weathering processes. As in the ore district of Panasqueira (Domingos & Pereira, 2018), some rocks in this studied region present a high (Sch S1) to moderate (EM and RE granites) degree of weathering capable of producing a porosity favourable to the ability of release the radon available for transport from the rocks to the subsoil (Tab. II). Thus it becomes essential to monitor the pathway of radon from rocks until reaching the confined spaces.

The distance to the first-order fracturing network *versus* indoor radon measurements was projected to understand the effect of geochemical, anthropogenic and structural control on the concentration of radon in dwellings (Fig. 5a). Thus, for faults to be considered the main pathways of radon conduction to the surface, a greater distance to residential areas would imply a lower concentration of indoor radon.

The effect of geological structures on the upward of radon into confined spaces is not proven. However, the indoor radon concentrations above the reference level of Portuguese legislation (^{222}Rn= 300 Bq/m^3; Decree-law 108/2018) occurs at a considerable distance from the regional fractures (above 300 meters), which indicates a geochemical or anthropogenic control (Fig. 5a). Just because large-scale fracturing records were used, a more detailed study of small-scale fracturing would be necessary and could prove in more detail the structural control over the radon upward to the surface. Besides, the geochemical and anthropogenic control over the indoor radon was much more noticeable; even when dwellings are mostly located on shists (Fig. 5b). Furthermore, in this region, the impact of geochemical and anthropogenic control stands out from the structural (R^2 = 0.63; Fig. 5a).

In this previous scenario, it is expected exceptional levels of radon in confined spaces from geochemical and anthropogenic control.

Indoor radon exposure

An atypical increase in the amount of radon available for transport in the rocks of the ore district of Ervedosa is expected due to the mobilization of uranium, in contrast with human habits and the watertight construction characteristics of the dwellings. Thus, it can provide a reliable estimation of the geogenic and anthropogenic contribution for indoor radon concentrations. This cause-effect relationship between uranium mobilization and the potential for radon production in rocks was also reported in the Panasqueira ore province (Domingos & Pereira, 2018). The residential areas of Ervedosa located in the schist S2 together with EM granite from the locality of Soutilha have a more remarkable geometric mean in the indoor radon concentration (Fig. 6a). The significant impact of geochemical control, it is once again confirmed (through the uranium content of these rocks, Fig. 4b) on the risk of exposure to radon in confined spaces (Fig. 6a). Hence, a higher risk of radon exposure is expected in the ore district, where the average of indoor radon concentrations are respectively 195, 196, 857 and 426 Bq·m^{-3} for dwellings located in S1, RE, S2 and EM lithologies (Fig. 6b e Tab. III). Even so, these average of indoor radon concentration obtained for these studied granitic areas were

lower than others from Northern Portugal, namely at Vila Pouca de Aguiar (Martins et al., 2016), Vila Real (Gomes et al., 2011) and Amarante (Martins et al., 2013).

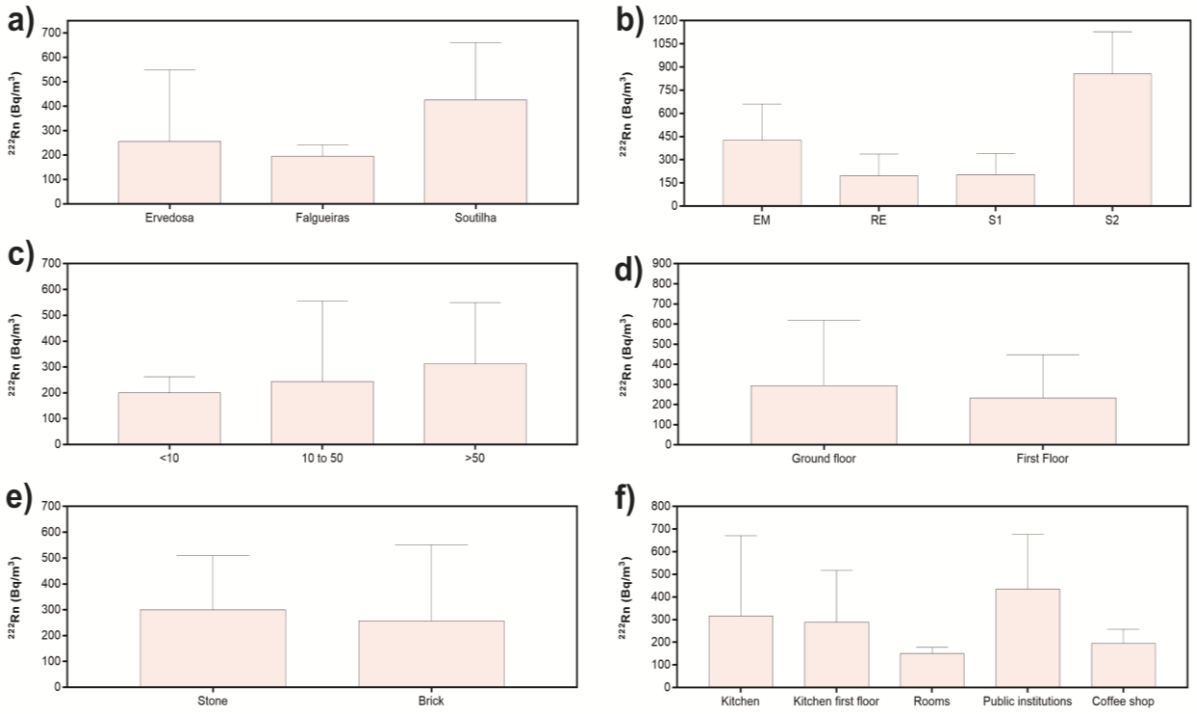

Figure 5 - 222Rn versus distance to fractures: a. geochemical, structural and anthropogenic control; b. with the percentage of studied lithologies.

A higher average of indoor radon was also found for older dwellings (>50 years; Fig. 6c). The dwellings with older construction stand out due to the occurrence of anomalous concentrations of residential radon located in the granite EM and Sch S2. Furthermore, these results may be more recurrent, mainly due to the Portuguese program to support more sustainable energy-efficient buildings (RCM nº 41/2020 and RCM nº 53/2020). Thus, the reconstruction of energy-efficient old dwellings will be increasingly supported by the Portuguese government through the use of watertight construction methods, including double-glazed windows and a roof on the outside walls.

It is also important to mention that these indoor radon results were collected during the winter and did not represent the annual average. During the winter period, residential radon concentrations are usually higher due to the use of fireplaces and human habits that disrupt natural ventilation. Furthermore, dwellings with ground floor, constituted by walls composed of rock into public institutions and kitchen division present the highest average of residential radon (Fig. 6d-f). Of the 46 studied dwellings, 15 exceeded the reference limit of Portuguese legislation (222Rn= 300 Bq·m-3), representing 33% of the total sampled buildings. There is also an increased concern in 2 dwellings with radon concentrations above 1000 Bq·m-3, with a maximum level of 1307 Bq·m-3.

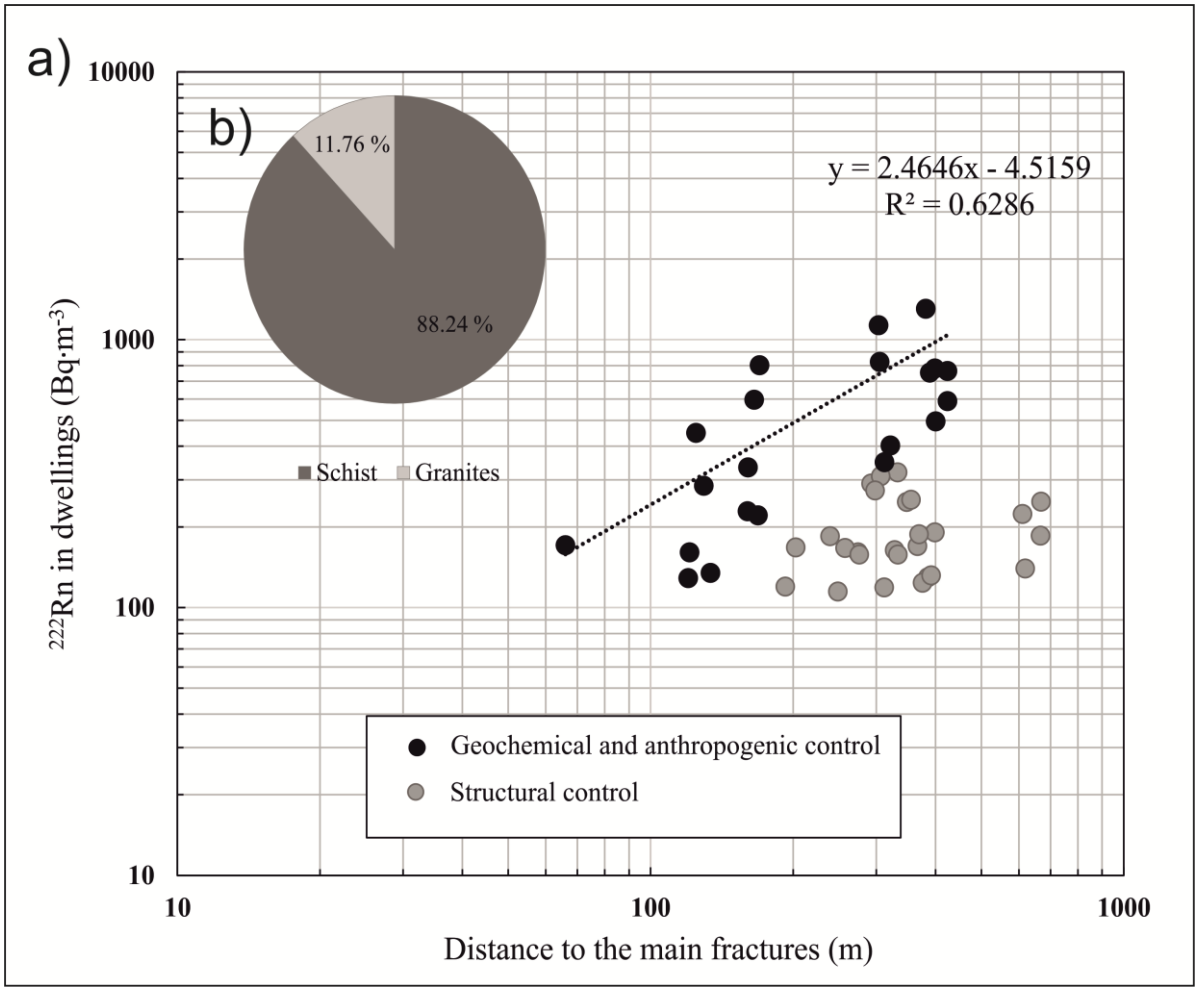

Figure 6 - Variation of indoor ^{222}Rn. a. localities. b. lithologies. c. dwellings age. d. ground or 1st Floor. e. construction materials. f. rooms divisions.

The geometric mean of the indoor radon in the studied lithologies coincides with the radiometric background. It is once again confirmed the geochemical control in the radon upward to the surface and subsequent entry into indoor air (Tab. III). Nevertheless, the geometric mean of radon activity from dwellings of Ervedosa ore district shows a large variance, which can be mainly attributed to the influence of geogenic and anthropogenic features. These crucial factors increase the vulnerability of human health by raising the indoor radon of favourable pathways from the source uranium-rich bedrock units to the surface including human habits and constructive housing methods (Groves-Kirkby et al., 2010; Drolet & Martel, 2016; Sferle et al., 2020; Yarmoshenko et al., 2016).

Neves et al. (2003) consider that the increased ventilation of dwellings during the summer provides, on average, a 37 % reduction in radon levels with those observed in the winter. Thus, the estimated annual mean of indoor radon for Ervedosa village is 338 Bq m^{-3}, exceeding the values presented by Dubois (2005) under the scope of radon survey performed in European countries.

Table III - The geometric mean of indoor radon concentrations with the corresponding average of outdoor dose rate.

Locality	Lithology	Indoor radon ($Bq \cdot m^{-3}$)	Dose (ηGy/h)	Total (cps)
Ervedosa	S1 schist	195	398	169
Ervedosa	S2 schist	857	687	884
Ervedosa	RE granite	196	421	211
Falgueiras	S1 schist	195	398	169
Soutilha	EM granite	426	359	194

Conclusions

The petrographic and geochemical characteristics of EM granite fulfill the requirements of fertile uraniferous granites. Micro-scale observations proved to be crucial for previously revealing the complexity of geochemical behaviour of uranium minerals and their migration through regional structures. The alteration indices showed that the weathering processes that occurred in the metamorphic halo might be the main factor that contributed to the mobilization of uranium from the surrounding granites to Sch S2. The importance of structural control has not been proven in upward of radon to the surface.

Concerning external radiation exposure, it is noticeable that the average gamma absorbed dose rates for all studied granites are, in general above, those determined for CIZtypical granites (ca. 200 ηGy/h). This study also show that buildings on the first floor with less than 50 years old, and brick walls present the lowest indoor radon average. In the sampled dwellings, the kitchens and public institutions tend to yield the highest indoor radon average concentrations, probably the first by the use of fireplaces, and the second because are located close to the uranium mineralized schist S2.

There is a strong correlation between geochemical and anthropogenic control (namely whole-rock uranium content and human habits) and indoor radon concentrations. This relation is particularly evidenced in schist S2 and EM granite, which are promptly able to raise indoor radon concentrations above the recommended limits. Overall, radon activity from dwellings of Ervedosa ore district shows a large variance, which can be mainly attributed to the influence of geogenic and anthropogenic characteristics, such as the local geology and not using natural ventilation during the winter period from human habits. Thus, corrective and preventive measures should be safeguarded by the APA (Agência Portuguesa do Ambiente, in Portuguese) for the risk of exposure to indoor radon in areas considered to be at higher risk, such as the region studied. As in other areas of the Portuguese territory, should not be overlooked other specific places in Portugal with uranium anomalies. In this way, these areas of most significant risk must be appropriately signalled and monitored by approving authorities.

The Portuguese radon plan must be urgently framed within the scope of new policies to encourage efficient construction, because of the harmful effect on human health due to the accumulation of radon

in indoor air. Land-use planning policies must also be efficient to apply new construction solutions, safeguarding the licensing of new buildings.

Acknowledgements: The authors acknowledge the financial and technical support provided by the Laboratory of Natural Radioactivity the Department of Earth Sciences (University of Coimbra, Portugal) and the Project ReNATURE - Valorization of the Natural Endogenous Resources of the Centro Region (Centro 2020; Centro-01-0145-FEDER-000007, Portugal). LMOM is integrated into CITAB research centre, financed by the FEDER/COMPETE/POCI - Operational Competitiveness and Internationalization Programme, under Project POCI-01-0145-FEDER-006958, and National Funds of FCT - Portuguese Foundation for Science and Technology, through the project UID/AGR/04033/2020. For the author integrated into the CITEUC, the research was additionally supported by National Funds of FCT - Portuguese Foundation for Science and Technology, under the project UID/QUI/00616/2020.

References

Adinsoft, S. (2010). XLSTAT-software, version 10. In *Addinsoft*.

Beaulieu, E., Goddéris, Y., Donnadieu, Y., Labat, D., & Roelandt, C. (2012). High sensitivity of the continental-weathering carbon dioxide sink to future climate change. *Nature Climate Change*, *2*(5), 346-349.

BEIR VI - Committee on Health Risks of Exposure to Radon (1999). *Health effects of exposure to radon*. Washington DC: National Academy Press.

Brown, G. C., Hughes, D. J., & Esson, J. (1973). New X.R.F. data retrieval techniques and their application to U.S.G.S. standard rocks. *Chemical Geology*, *11*, 223-229.

Cambon, A. R. (1994). Uranium Deposits in Granitic Rocks. In *Notes on the National Training Course on Uranium Geology and Exploration*. Cairo: IAEA and NMA.

Cosma, C., Cucoş-Dinu, A., Papp, B., Begy, R., & Sainz, C., (2013). Soil and building material as main sources of indoor radon in Băiţa-Ştei radon prone area (Romania). *Journal of Environmental Radioactivity*, *116*, 174-179.

Cosma, C., Papp, B., Cucoş-Dinu, A., & Sainz, C. (2015). Testing radon mitigation techniques in a pilot house from Băiţa-Ştei radon prone area (Romania). *Journal of Environmental Radioactivity*, *140*, 141-147.

Costa, M. R., Pereira, A. J. S. C., Neves, L. J. P. F., & Ferreira, A. (2017). Potential human health impact of groundwater in non-exploited uranium ores: The case of Horta da Vilariça (NE Portugal). *Journal of Geochemical Exploration*, *183*, 191-196.

Darnley, A. G. (1982). “Hot Granites” Some General Remarks. In Y. J. Maurice (Ed.), *Uranium in Granites*. Paper No. 81-23 (pp. 1-10). Ottawa: Geological Survey of Canada.

Darby, S., Hill, D., Auvinen, A., Barros-Dios, J. M., Baysson, H., Bochicchio F., … Deo, H. (2005).

Radon in homes and risk of lung cancer: collaborative analysis of individual data from 13 European case-control studies. *BMJ*, *330*(223). https://doi.org/10.1136/bmj.38308.477650.63

Domingos, F., & Pereira, A. (2018). Implications of alteration processes on radon emanation, radon production rate and W-Sn exploration in the Panasqueira ore district. *Science of the Total Environment*, *622-623*, 825-840.

Dubois, G. A. G. (2005). An overview of radon surveys in Europe. *Scientific and Technical Research Series, EUR 21892 EN*. Luxembourg: Joint Research Centre of the European Commission.

Drolet, J. P., & Martel R. (2016). Distance to faults as a proxy for radon gas concentration in dwellings. *Journal of Environmental Radioactivity*, *152*, 8-15.

Dupré, B., Dessert, C., Oliva, P., Goddéris, Y., Viers, J., François, L., … Gaillardet, J. (2003). Rivers, chemical weathering and Earth's climate. *Comptes Rendus Geoscience*, *335*(16), 1141-1160.

EPA (2003). *EPA Assessment of risk from radon in homes. EPA 402-R-03-003*. Washington DC: United States Environmental Protection Agency.

ESRI (2010). *ArcMap (Version 10).* Lisboa: ESRI Portugal.

Fawzy, K. M. (2017). Characterization of a post orogenic A-type granite, Gabal El Atawi, Central Eastern Desert, Egypt: Geochemical and radioactive perspectives. *Open Journal of Geology*, *7*, 93-117.

Fedo, C. M., Nesbitt, H. W., & Young, G. M. (1995). Unravelling the effects of potassium metasomatism in sedimentary rocks and paleosols, with implications for paleoweathering conditions and provenance. *Geology*, *23*(10), 921-924.

Gomes, M. E. P., & Neiva, A. M. R. (2002). Petrogenesis of Tin-bearing Granites from Ervedosa, Northern Portugal: The Importance of Magmatic Processes. *Geochemistry*, *62*(1), 47-72.

Gomes, M. E. P., & Neiva, A. M. R. (2005). Geochemistry of granitoids and their minerals from Rebordelo–Agrochão area, northern Portugal. *Lithos*, *81*(1-4), 235-254.

Gomes, E., Neves, L., Coelho, F., Carvalho, A., Sousa, M., & Pereira, A. (2011). Geochemistry of granites and metasediments of the urban area of Vila Real (Northern Portugal) and correlative radon risk. *Environmental Earth Sciences*, *64*(2), 497-502.

Groves-Kirkby, C. J., Denman, A. R., Phillips, P. S., Crockett, R. G. M., & Sinclair, J. M. (2010). Comparison of seasonal variability in European domestic radon measurements. *Natural Hazards and Earth System Science*, *10*(3), 565-569.

Harnois, L. (1988). The CIW index: A new chemical index of weathering. *Sedimentary Geology*, *55*(3-4), 319-322.

Lécolle, M., Derré, C., Noronha, F., Roger, G.: (1981). *Distribution des concentrations Sn-W dans le Nord du Trás-os-Montes (Portugal). Typologies gîtologiques et minéralogiques*. *Rapport final de l'ATP 35.48, "Formation et distribution des gisements"*. ATP-CNRS Action thématique programmée du Centre National de la Recherche Scientifique. Paris: CNRS

Limpo de Faria, F. (1966). Gites d'uranium portugais dans des formations metasedimentaires. *Comunicações Dos Serviços Geológicos de Portugal*, *50*, 9-50.

Martins, L. M. O., Gomes, M. E. P., Neves, L. J. P. F., & Pereira, A. J. S. C. (2013). The influence of geological factors on radon risk in groundwater and dwellings in the region of Amarante (Northern Portugal). *Environmental Earth Sciences*, *68*(3), 733-740.

Martins, L. M. O., Gomes, M. E. P., Teixeira, R. J. S., Pereira, A. J. S. C., & Neves, L. J. P. F. (2016). Indoor radon risk associated to post-tectonic biotite granites from Vila Pouca de Aguiar pluton, northern Portugal. *Ecotoxicology and Environmental Safety*, *133*, 164-175.

McLennan, S. M., Hemming, S., McDaniel, D. K., & Hanson, G. N. (1993). Geochemical approaches to sedimentation, provenance, and tectonics. *Geological Society of America Special Papers*, *284*, 21-40.

Neiva, J. M., & Matos Dias, J. M. (2010). Mineralization and genesis of Portuguese uranium deposits. In J. M. C. Neiva, A. Ribeiro, L. M. Víctor, F. Noronha, F., & M. Ramalho, M. (Eds.), *Ciências Geológicas: Ensino, investigação e a sua história, vol. II - Geologia Aplicada,* (pp. 109-119). Braga: Associação Portuguesa de Geólogos and Sociedade Geológica de Portugal.

Nesbitt, H. W., & Young, G. M. (1982). Early proterozoic climates and plate motions inferred from major element chemistry of lutites. *Nature*, *299*, 715-719.

Nesbitt, H. W., & Young, G. (1984). Prediction of some weathering trends of plutonic and volcanic rocks based on thermodynamic and kinetic considerations. *Geochimica et Cosmochimica Acta*, *48*(7), 1523-1534.

Neves, L. J. P. F., Avelans, S. C. C., & Pereira, A. J. S. C. (2003). Seasonal variation radon gas in dwellings in the urban area of the Guarda (Central Portugal), In. *Proceedings of the IV Iberian Congress of Geochemistry, XIII Week Geochemistry*, (pp. 307-309). Coimbra: Sociedade Geológica de Portugal.

Parker, A. (1970). An Index of Weathering for Silicate Rocks. *Geological Magazine*, *107*(6), 501–504.

Pereira A., Lamas, R., Miranda; M., Domingos, F., Neves, L., & Costa L. (2017). Estimation of the radon production rate in granite rocks and evaluation of the implications for geogenic radon potential maps: A case study in Central Portugal. *Journal of Environmental Radioactivity*, 166(2), 270-277.

Pereira, A. J. S. C., Pereira, M. D., Neves, L. J. P. F., Azevedo, J. M. M., & Campos, A. B. A. (2015). Evaluation of groundwater quality based on radiological and hydrochemical data from two uraniferous regions of Western Iberia: Nisa (Portugal) and Ciudad Rodrigo (Spain). *Environmental Earth Sciences*, *73*(6), 2717-2731.

Prazeres, C. M., Batista, M. J., Pinto, A. J., & Gonçalves, M. A. (2018). Uranium distribution and mobility in the weathering zone of the Nisa deposit, Portugal. *Journal of Iberian Geology*, *44*(3), 497-512.

Price, J. R., & Velbel, M. A. (2003). Chemical weathering indices applied to weathering profiles developed on heterogeneous felsic metamorphic parent rocks. *Chemical Geology*, *202*(3-4), 397-416.

Ribeiro, A. (1990). Part IV – Central-Iberian Zone. Introduction. In R. D. Dallmeyer, & E. Martinez

Garcia, (Eds.). *Pre-Mesozoic Geology of Iberia* (pp. 143-144). Berlin and Heidelberg: Springer-Verlag.

Sferle, T., Dobrei, G., Dicu, T., Burghele, B.-D., Brişan, N., Cucoş (Dinu), A., … Sainz, C. (2020). Variation of indoor radon concentration within a residential complex. *Radiation Protection Dosimetry*, *189*(3), 279-285.

Sharma, A., & Rajamani, V. (2000). Major element, REE, and other trace element behavior in amphibolite weathering under semiarid conditions in Southern India. *The Journal of Geology*, *108*(4), 487-496.

Talavera, M. G., García Perez, A., Rey, C., & Ramos, L. (2013). Mapping radon-prone areas using radiation dose rate and geological information. *Journal of Radiological Protection*, *33*(3), 605-620.

Tartèse, R., Boulvais, P., Poujol, M., Gloaguen, E., & Cuney, A. (2013). Uranium Mobilization from the Variscan Questembert Syntectonic Granite During Fluid-Rock Interaction at Depth. *Economic Geology*, *108*(2), 379-386.

WHO (2010). *Guidelines for Indoor Air Quality: Selected pollutants, 2010*. Copenhagen: World Health Organization, Regional Office for Europe.

Yarmoshenko, I., Malinovsky, G., Vasilyev, A., Onischenko, A., & Seleznev, A. (2016). Geogenic and anthropogenic impacts on indoor radon in the Techa River region. *Science of the Total Environment*, *571*, 1298-1303.

Young, R. G. (1984). Uranium deposits of the world, excluding Europe. In de Vivo, B. (Ed.), *Uranium geochemistry, mineralogy, geology, exploration and resources* (pp. 117-139). Berlin: Springer.